Received: 6 August 2019 | Revised: 5 May 2020 | Accepted: 8 June 2020

DOI: 10.1002/hbm.25101

RESEARCH ARTICLE

WILEY

Invasive versus non-invasive mapping of the motor cortex

Carolin Weiss Lucas[1] | Charlotte Nettekoven[1] | Volker Neuschmelting[1] | Ana-Maria Oros-Peusquens[2] | Gabriele Stoffels[2] | Shivakumar Viswanathan[2] | Anne K. Rehme[2,3] | Andrea Maria Faymonville[1] | N. Jon Shah[2,4] | Karl Josef Langen[2] | Roland Goldbrunner[1] | Christian Grefkes[2,3]

[1]Medical Faculty and University Hospital, Center for Neurosurgery, University of Cologne, Cologne, Germany

[2]Research Centre Jülich, Institute of Neuroscience and Medicine, Jülich, Germany

[3]Medical Faculty and University Hospital, Department of Neurology, University of Cologne, Cologne, Germany

[4]Department of Neurology, RWTH Aachen University, University Clinic Aachen, Aachen, Germany

Correspondence
Carolin Weiss Lucas, Klinik für Allgemeine Neurochirurgie. Uniklinik Köln, Bettenhaus Eb. 8. Kerpener Str. 62. 50931 Cologne, Germany.
Email: carolin.weiss@uk-koeln.de

Funding information
Deutsche Forschungsgemeinschaft, Grant/Award Number: INST 1856/50-1; University of Cologne, Faculty of Medicine, Grant/Award Number: Koeln Fortune Gerok 8/2016

Abstract

Precise and comprehensive mapping of somatotopic representations in the motor cortex is clinically essential to achieve maximum resection of brain tumours whilst preserving motor function, especially since the current gold standard, that is, intraoperative direct cortical stimulation (DCS), holds limitations linked to the intraoperative setting such as time constraints or anatomical restrictions. Non-invasive techniques are increasingly relevant with regard to pre-operative risk-assessment. Here, we assessed the congruency of neuronavigated transcranial magnetic stimulation (nTMS) and functional magnetic resonance imaging (fMRI) with DCS. The motor representations of the hand, the foot and the tongue regions of 36 patients with intracranial tumours were mapped pre-operatively using nTMS and fMRI and by intraoperative DCS. Euclidean distances (ED) between hotspots/centres of gravity and (relative) overlaps of the maps were compared. We found significantly smaller EDs (11.4 ± 8.3 vs. 16.8 ± 7.0 mm) and better spatial overlaps (64 ± 38% vs. 37 ± 37%) between DCS and nTMS compared with DCS and fMRI. In contrast to DCS, fMRI and nTMS mappings were feasible for all regions and patients without complications. In summary, nTMS seems to be the more promising non-invasive motor cortex mapping technique to approximate the gold standard DCS results.

KEYWORDS

brain tumours, electric stimulation, functional magnetic resonance imaging, glioma, precentral motor area, surgical procedures, neurologic, transcranial magnetic stimulation

Abbreviations: APB, abductor pollicis brevis muscle; BOLD, blood oxygenation level dependent; CoG, centre(s) of gravity; DCS, direct cortical stimulation; ED, Euclidean distance(s); EPI, echo planar imaging; FDR, false-discovery-rate; FMRI, functional MRI; FWE, family-wise error; GTR, gross total resection; KPS, Karnofsky performance scale; MC, motor cortex; MEG, magnetoencephalography; MEP, motor-evoked potential; NIfTI, neuroimaging informatics technology initiative; nTMS, neuronavigated transcranial magnetic stimulation; RMT, resting motor threshold; SEM, standard error of the mean; SPM, statistical parametric mapping.

Carolin Weiss Lucas, Charlotte Nettekoven, Roland Goldbrunner and Christian Grefkes contributed equally to this work (shared first/last authorship).

1 | INTRODUCTION

The achievement of total tumour resection whilst preserving motor function is the major objective when removing brain tumours located in or close to functionally important brain areas. Especially in cases of functional reorganisation as a result of brain plasticity, which is a common finding in brain tumours close to eloquent locations, the extent

of the functional representation is often not delineated by anatomical landmarks for example, the precentral gyrus for the motor cortex (MC) (see Duffau, 2014 for review). Therefore, to assure postoperative functional integrity, intraoperative cortex mapping and monitoring of motor functions by intraoperative direct cortical stimulation (DCS) has become a crucial part of surgical procedure over the last decades, and is widely accepted as the gold standard (see Desmurget & Sirigu, 2015 for review). DCS ensures a precise investigation of cortical function. However, intraoperative mapping does not allow for a-priori assessment of the function-lesion relationship and, thus, cannot be readily integrated in the preoperative decision-making. Moreover, DCS requires a rigorous anaesthesiological regime (see Bonhomme, Franssen, & Hans, 2009 or review) and suffers from a series of limitations linked to the intraoperative setting. In particular, reliable functional mapping can be impeded by the surgical access, for example, bridging veins next to the midline, time pressure, or the absence/loss of motor evoked potentials (MEP), mostly due to the influence of anaesthetics. Limited feasibility of DCS regarding a comprehensive mapping of the motor representation may impact on the functional outcome since not only complete but also partial lesions of motor areas can cause relevant surgery-related deficits (Gil-Robles & Duffau, 2010). On the other hand, an optimised extent of tumour resection is highly important with respect to prognosis and overall survival. Therefore, obtaining a detailed functional map of eloquent areas like the MC is of particular clinical interest. Importantly, obtaining such information prior to surgery allows a better preoperative risk evaluation and surgery planning (Rosenstock et al., 2017).

In the past, functional magnetic resonance imaging (fMRI) and magnetoencephalography (MEG) or a combination of both methods (Gallen et al., 1995; Kober et al., 2001; Korvenoja et al., 2006) as well as [^{15}O]-H_2O positron emission tomography (water-PET; Deiber et al., 1991; Reinges et al., 2004) have been used for the non-invasive localization of the MC. More recently, neuronavigated transcranial magnetic stimulation (nTMS) has gained increasing acceptance for preoperative localization of the MC (Lefaucheur & Picht, 2016 for review). High spatial precision within a few millimetres range and limited dependence on the compliance of the patient have driven interest in nTMS for pre-operative brain mapping (Takahashi, Vajkoczy, & Picht, 2013 for review). Previous studies compared the cortical localization of the MC map centres of the upper and lower extremities assessed by nTMS to intraoperative DCS and to MEG whereas thus far two pilot studies (n = 7–9 participants) compared both nTMS and fMRI to DCS map centres. However, data are scarce with respect to differences in spatial extents although a precise and comprehensive delineation of the functional representation is of high clinical importance. Moreover, non-invasive mapping of other functionally important motor regions for example, the face representation has not been validated at all using DCS, despite its clinically highly relevant role in articulation and swallowing.

In order to provide a comprehensive evaluation of non-invasive presurgical mapping techniques, we compared both nTMS and fMRI to the gold standard monopolar DCS with respect to the face, the hand, and the foot representations—intending to approximate the primary motor region. Beyond comparing the centre coordinates of the respective body part representations, we also evaluated the spatial extent of all somatotopic maps and took the feasibility and motor outcome into account. We hypothesised that, due to the accumulating imprecision in space inherent to function localization models, the neuronavigation systems involved and the brain shift after dural opening, none of the two non-invasive methods would allow for a perfect match with functional maps assessed by DCS. However, we expected a better agreement of nTMS with DCS due to their similarity in how the mapping is achieved, that is, by stimulating corticospinal neurons through a relatively focal electric field compared with the vascular signal recorded by fMRI.

2 | MATERIALS AND METHODS

A consecutive series of patients with intracranial tumours were investigated by nTMS and fMRI prior to surgery. The extent of the MC and the localization of the functional centres were validated intraoperatively by neuronavigated, monopolar DCS. The study was approved by the local Ethics committee. Written informed consent was obtained from all study participants.

2.1 | Patients

Thirty-six patients (Table 1) scheduled for microsurgical removal of intracranial tumours adjacent to or involving the precentral gyrus and/or the corticospinal tract were prospectively enrolled between 2011 and 2013. All patients were able to care for themselves (Karnofsky performance scale [KPS] ≥ 70%; Karnofsky & Burchenal, 1949). Epilepsy was not generally considered as a contraindication for single-pulse nTMS due to its high clinical relevance and the low procedural risk (Tarapore et al., 2016). The study was approved by the local ethics committee and was carried out according to the declaration of Helsinki (revised 2013).

2.2 | Clinical outcome assessment

The severity of motor deficits for the extremities (the face) was classified using two semi-quantitative ratings adopted from the Medical Research Council (MRC) scale for muscle strength of the arms or legs (Medical Research Council, 1976) and the facial palsy scale introduced by House and Brackmann (1985), which were both developed for peripheral nervous system pathologies. Deficits were classified accordingly based on at least one muscle group: (a) mild = 4/5 on the MRC scale for muscle strength of the arms or legs; for facial palsy: grade II according to House and Brackmann (1985), without relevant functional deficit affecting daily life (KPS 90–100%); (b) moderate = 3/5 on the MRC scale (House-Brackmann °III), moderately affecting normal activity (KPS 80%); (c) severe = 0–2/5 on the MRC scale

TABLE 1 Patient characteristics

Attribute	Phenotype	*n* (percentage)
Gender	Male	21 (58%)
	Female	15 (42%)
Handedness	Right	32 (89%)
	Left	4 (11%)
Motor deficit	No	17 (47%)
	Yes	19 (53%)
Severity	Mild	11 (53%)
	Moderate	6 (32%)
	Severe	2 (16%)
Predominant manifestation	Brachiofacial	15 (79%)
	Leg	4 (21%)
Tumour entity	Glioma	26 (72%)
	Glioblastoma WHO IV°	18 (69%)
	Glioma WHO III°	6 (23%)
	Glioma WHO II°	2 (8%)
	Others	10 (28%)
	Carcinoma metastasis	6 (60%)
	Meningioma	3 (30%)
	B-cell lymphoma	1 (10%)
Tumour stage	First diagnosed	30 (83%)
	Recurrence	6 (17%)
Tumour hemisphere	Left	14 (39%)
	Right	22 (61%)
Tumour localisation	Precentral	19 (53%)
	Postcentral	11 (31%)
	Lateral frontoparietal region	6 (17%)

(House-Brackmann °IV–VI), strongly affecting normal activity (KPS ≤70%). Accordingly, deterioration in motor function was defined as a decrease in at least one point/grade on the MRC or the House-Brackmann scale. Of note, the degree of facial palsy was assessed instead of the tongue force due to better rateability and the existence of a standardised grading system whereas for fMRI and nTMS exams of the functional representation, the tongue function/muscle was used rather than facial muscles due to better technical feasibility and—at the same time—substantial overlap between cortical face muscle and tongue representations (e.g., Weiss et al., 2013; Catani, 2017 for review).

2.3 | Functional MRI

2.3.1 | Acquisition

The functional MRI (fMRI) data were acquired using a gradient echo planar imaging (EPI) sequence sensitive to detect blood oxygenation level dependent (BOLD) changes in tissue contrast (261 EPI volumes, repetition time = 2000 ms; cf. Weiss Lucas et al., 2017). T1 volumes (Magnetization Prepared Rapid Acquisition Gradient Echo) without contrast agent served as the anatomical reference scan for fMRI processing. All MRI measurements were obtained from a 3T MR scanner (MAGNETOM Trio, Siemens Healthcare, Erlangen, Germany).

2.3.2 | Task

The fMRI task (block design) was designed to elicit activations associated with movements of the same muscles used for nTMS (see below) contralateral to the side of the brain tumour. Subjects performed visually paced (1.5 Hz) alternating movements with the thumb, the toes or the tongue in a randomised order (block length = 16 s incl. 2 s instruction; four repetitions per body part, total task duration = 4:16 min; cf. Weiss Lucas et al., 2017). Movement blocks were separated by an equal number of resting baselines (block length = 15 s), in which subjects saw a black screen and a white fixation cross until an instruction text indicated the next body part to move. Task performance was controlled by an investigator inside the scanner room. The entire fMRI scanning protocol lasted 8:30 min.

2.3.3 | Pre-processing and statistics

The MRI volumes were pre-processed and statistically modelled using the Statistical Parametric Mapping software package (SPM 8; Wellcome Department of Imaging Neuroscience, London, UK, http://www.fil.ion.ucl.ac.uk) implemented in Matlab (version 2009a, The MathWorks Inc., MA). Pre-processing (realignment, co-registration, smoothing) was achieved using default parameters (including an isotropic Gaussian kernel of 8 mm full width at half maximum). For single subject analyses, voxels were considered significantly activated when passing a threshold of T = 4.59 ($p < .05$; family-wise error [FWE] corrected at the voxel level). Whenever necessary (no sufficient activation using FWE correction in the precentral gyrus), the threshold was lowered to an uncorrected level of $p < .05$. This affected the following number of subjects: hand: $n = 13$, foot: $n = 7$, tongue: $n = 4$. For one patient, even at this liberal threshold no sufficient tongue activation could be detected. The somatotopic functional cluster of interest was chosen according to the highest BOLD activity in the left precentral gyrus, thereby adopting a similar approach as in nTMS (Figure 1). In case of multiple local maxima within one cluster, for example, also on the neighbouring postcentral gyrus, the highest maximum in the precentral gyrus was used for further processing.

2.4 | nTMS

nTMS was performed using a standard biphasic stimulation device equipped with a 70 mm figure-of-eight coil and a neuronavigation system (NBS 4.2, Nexstim Ltd., Helsinki, Finland). After EMG electrode placement and co-registration of the patients' head, the somatotopic

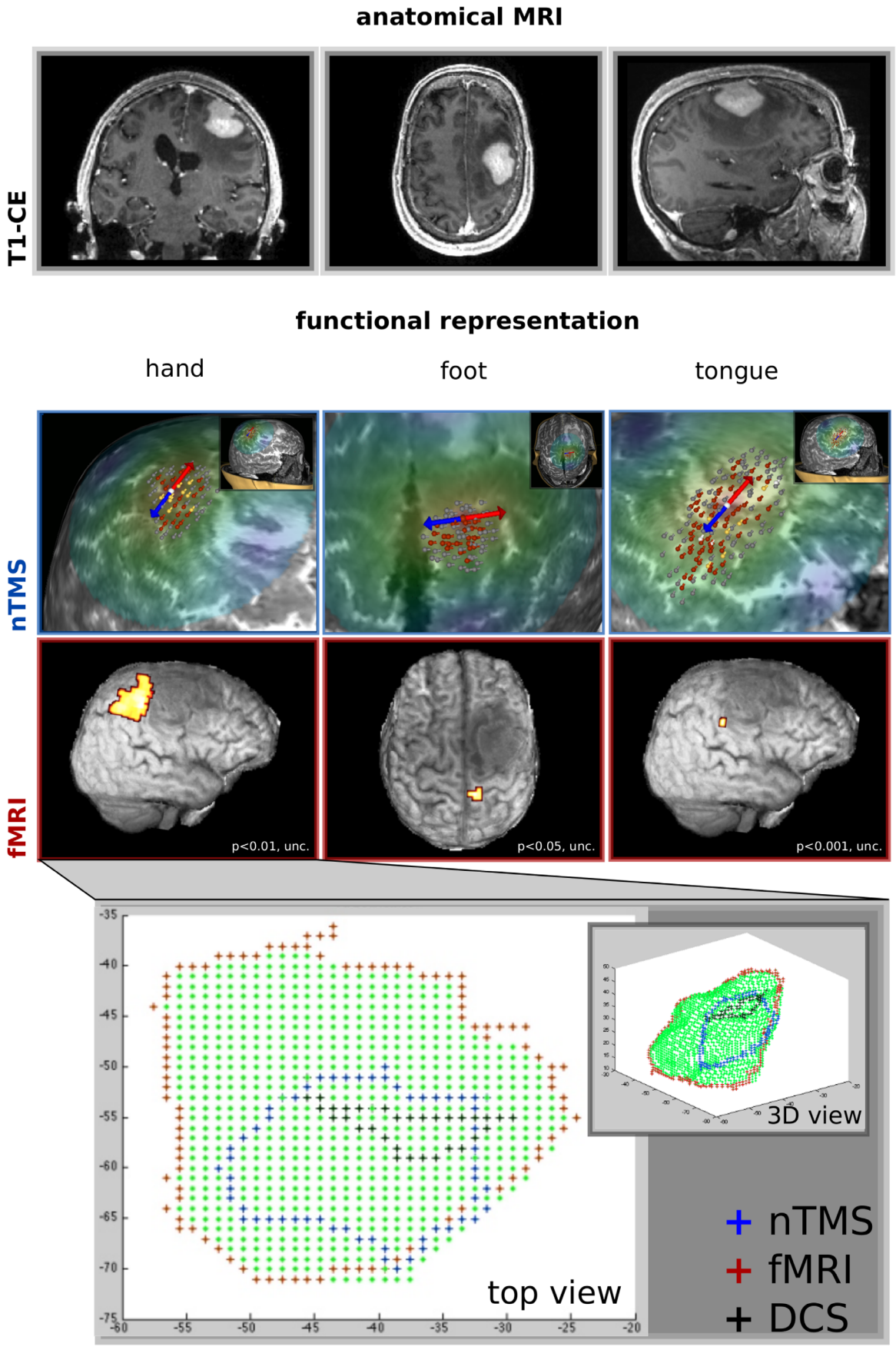

FIGURE 1 Legend on next page.

MC representations in the vicinity of the tumour were mapped (see *Mapping procedure*). The total mapping duration was 60–120 min.

2.4.1 | EMG

MEPs were recorded from the abductor pollicis brevis muscle (APB), the medial plantar toe flexor muscles and the anterior lateral tongue muscles contralateral to the side of the brain tumour using surface electrodes (Ambu Neuroline, Bad Nauheim, Germany). The areas of interest were chosen according to the tumour anatomy and the planned craniotomy size, that is, all areas neighbouring the tumour and/or to be exposed during surgery were mapped.

2.4.2 | Mapping procedure

Mapping was performed using a standard stimulation intensity of 110% of the resting motor threshold (RMT; see for example, Weiss et al., 2013). The RMT was separately determined for the "hotspot" of each muscle representation. Whenever involuntary pre-innervation was observed in the EMG traces, which can lead to "artificial" increase of MEPs and thus reduce specificity, stimulation trials were excluded from further analysis for the foot and the hand representation. For mapping the tongue area, voluntary contraction was occasionally (n = 5) required to reduce excitability thresholds in order to prevent direct nerve stimulation and/or discomfort. For each muscle representation, 120–200 pulses were applied with stable coil orientation (Figure 1) using a grid projected onto the brain surface rendering during the mapping (5 mm spacing between grid nodes; 2–3 stimulations per grid square unit). The outer margin of a given functional area was determined by two adjacent negative responses.

2.5 | DCS

Surgery was performed under general analgo-anaesthesia using propofole and sufentanil (Scheufler & Zentner, 2002; see also Sloan, 1998 for review). Presurgical sedation was restricted to clonidine. Low doses of a short-lasting muscle relaxant (Atacurium) were only administered for intubation. Residual relaxant effects were excluded prior to DCS using relaxometry (see Hemmerling & Le, 2007 for review).

Standard EMG needles (Ambu® Neuroline) were placed into the muscles corresponding to the nTMS and fMRI protocols (APB, plantar toe flexors, lateral tongue). The acquired nTMS and fMRI centre coordinates were integrated into the neuronavigation software (iPlanNet®, Brainlab, Feldkirchen, Germany) and were visible via a screen inside the operation room. After co-registration of the patient's head and the rigid stimulation probe, craniotomy and durotomy were performed. For DCS, anodal rectangular pulses were applied (500 Hz, 500 μs; stimulator: Viasys ENDEAVOUR CR; Suess, Suess, Brock, & Kombos, 2006; Szelényi et al., 2010) using monopolar stimulation. DCS mapping started from the preoperatively acquired nTMS and fMRI hotspot coordinates, using an initial stimulation intensity of 10 mA. In case of negative MEP responses at both hotspots, stimulation intensity was increased in steps of 5 mA until reliable MEPs were acquired from at least one hotspot. In case of positive MEP responses at both hotspots, the threshold determination procedure was continued over the site (nTMS or fMRI hotspot) at which stronger MEPs were elicited. Second, a more precise threshold determination was performed: To this end, stimulation intensity was adjusted to the least stimulation intensity, at which an MEP >50 μV could be evoked in three out of five of the stimulation trains (max. 25 mA). After this, we assured that stimulation elsewhere (using the same stimulation intensity) did not lead to significantly better MEP responses; otherwise the motor threshold was readjusted. These first steps were applied to each accessible somatotopic representation. Finally, mapping of the respective region was performed at suprathreshold intensities (motor threshold +1 mA) from the centre outwards until no more reliable MEPs were evoked. Importantly, the map size was limited by the size of the craniotomy, the subarachnoidal space and superficial vessels such as bridging veins, especially when stimulating the foot representation. Of note, this common limitation of intraoperative DCS was not circumvented by enlarging craniotomy due to ethical reasons. For each simulation response, the MEP amplitude and the stimulation localization (using the 3D coordinate acquisition option implemented in the neuronavigation system) were obtained.

2.6 | Statistical and computational congruency measures

2.6.1 | Euclidean distances between hotspots and centres of gravity

The nTMS and the DCS hotspots were defined as the coordinates yielding the highest MEP amplitudes at rest while the fMRI local activation maximum represents the coordinate with highest t-value in a given functional area within the precentral gyrus. Moreover, we computed the centres of gravity (CoG) for each nTMS, fMRI and DCS map as a reliable measure for the map centre (Vidyasagar & Parkes, 2011). The distances of the respective coordinates obtained for the three

FIGURE 1 Example of somatotopic fMRI clusters and nTMS maps. **MC** representation of the hand, the foot and the tongue (from left to right) revealed by (a) nTMS (first row; coil/E-field orientation indicated by red part of the arrows; nTMS pulses represented by dots, coloured according to MEP amplitudes: <50 μV [grey]/50–200 μV [red]/201–1,000 μV [yellow]/>1,000 μV [white]) and (b) fMRI cluster analysis (second row; BOLD signal strength colour-encoded; after identification of the fMRI peak activation cluster in the precentral gyrus, all other voxels were removed from the individual SPM{T} map) in individual patients. The bottom section provides a schematic overview of the hand mapping results obtained using all three mapping techniques, projected onto the cortical surface (blue: nTMS; red: fMRI; black: DCS) [Color figure can be viewed at wileyonlinelibrary.com]

different mapping modalities were determined by calculating Euclidean distances (ED) in 3D single subject space. For better comparability, mapping data were projected onto the brain surface level using a custom-written Matlab script (see below).

2.6.2 | Spatial overlap volumes

Overlap volumes of the respective motor maps obtained by the three different modalities (nTMS, fMRI, DCS) were computed for each individual subject based on surface-projected data. All computations were performed using custom scripts written in MATLAB (Mathworks Inc.) and the open source toolbox "Tools for NIfTI and ANALYZE image" (Shen, 2014). Since the projected fMRI/nTMS coordinates and the DCS coordinates were located on the convoluted cortical surface, we sought to obtain a representative cortical area for each modality that compactly contained all the corresponding sampled points whilst respecting the surface geometry. First, a single-voxel grey-matter surface was obtained from each subject's anatomical scan using the program (*bet2*) implemented in the FSL software package (FMRIB Software Library v5.0.8, FMRIB, Oxford, UK; https://fsl.fmrib.ox.ac.uk/fsl/fslwiki). Next, the Cartesian coordinates of these extracted voxels and the sampled points for each modality were transformed to spherical coordinates. In the spherical θ-ψ coordinate space (where θ is the (azimuth) angle in the x-y plane relative to the x-axis, and ψ is the (elevation) angle relative to the x-y plane), we computed the smallest polygon (or convex hull [Preparata & Shamos, 1985]) that contained all the sampled points. At least three points were required to obtain a valid convex hull. Subsequently, all voxels on the cortical surface with θ-ψ coordinates lying strictly within this convex hull were defined as the representative cortical area for that modality. A graph-theoretic procedure was used to ensure that the voxels belonging to this area formed a single connected entity (see Figure 1 for examples). If this could not be achieved, the respective cortical area was excluded from further analysis (fMRI: 9%; DCS: 19% of areas).

Finally, for each subject, the spatial overlap between the different modalities (nTMS, fMRI, DCS) as well as the Dice coefficient—a measure to quantify the similarity of motor maps (Dice et al., 1945)—were calculated. The Dice coefficient ranges between 0 and 1, with 0 indicating no overlap and 1 indicating perfect overlap. There were no significant differences between the fMRI and nTMS map sizes within the hand, foot or tongue area ($p > .05$, FDR-corrected; Table S1), accompanied by a generally big interindividual variation regarding both nTMS and fMRI volumes (Table S2). Therefore, we assumed no significant influence of the nTMS versus fMRI activation volumes on the map overlaps/Dice coefficients. In contrast, to account for the relatively small area mapped by DCS as compared with both fMRI and nTMS ($p < .01$; Table S2) due to the size of the craniotomy, we calculated relative overlap volumes, that is, (nTMS∩DCS)/DCS versus (fMRI∩DCS)/DCS. Moreover, a semi-quantitative rating was performed to classify whether DCS data points were included completely versus partially versus not at all inside the margins of the nTMS or fMRI maps to assess the sensitivity of the non-invasive functional localizer methods with respect to DCS.

2.7 | Statistical analysis

The statistical analyses were performed using R (R Studio, Version 0.98.507). For multi-factorial analysis, n-factorial ANOVA were calculated. In case of normal data distribution, according to the Shapiro-Wilks test, post hoc paired *t*-tests were performed, otherwise Wilcoxon's signed rank test was used to compare the means between different subsets of the group. Semiquantitative (count) data were analysed as contingency tables with subsequent McNemar test for dependent variables and three categories (McNemar, 1947). Whenever necessary, correction for multiple comparisons was achieved by using the false-discovery-rate (FDR) approach (Benjamini & Hochberg, 1995). The person who performed the post-processing of fMRI and nTMS results was blinded to the DCS data. However, blinding the surgeon who acquired the DCS data, intraoperatively, to the fMRI and nTMS results was omitted since the functional localizer data were used for surgery planning as part of the standard of care.

The following assumptions were made for the a priori sample size calculation: we expected an at least medium effect size of Cohen's d = 0.8. To assure a statistical power of 0.8, the acquisition of at least $n = 33$ comparisons was planned, that is, pairwise comparisons of means (Effect size d = 0.5, alpha = 0.05, two-sided).

3 | RESULTS

3.1 | Patient characteristics and clinical outcome

Detailed characteristics of the 36 patients included in the study (58% male, mean age 56 ± 13 years, median KPS 90) are provided in Table 1. Gross total resection (GTR) could be achieved in 59% of the patients with intra-axial tumours according to post-operative structural MRI within 48 hr. In 62% of the remaining patients with residual tumour, the attempt of GTR was switched to a strategy of partial resection during surgery, due to (a) tumour adherence to delicate anatomical or vascular structures (46%) or (b) the DCS results showing eloquent motor cortex in the tumour infiltration zone (15%). Regarding postoperative motor function, 33% of the patients showed a deterioration of motor functions for more than 48 hr after surgery. However, only in 6% of the cases, this functional deterioration was major (i.e., moderate or severe; Table 1). Three percentage of the patients recovered fully until discharge, 15% of the patients within a few weeks afterwards. At 3 months after surgery, 15% of the patients presented with mild persistent postoperative deficits. Of note, the rate of postoperative functional deficits was independent from the technical feasibility of a comprehensive, intraoperative DCS mapping (DCS-failure [$n = 6$]: 33% vs. DCS-completed [$n = 30$]: 30%; $p = 1$).

3.2 | Tolerability and side effects

All procedures were generally well tolerated. Typical side effects of nTMS were mild headache in 24% of the subjects during the

examination. Prolonged headache (lasting for more than 10 min. After the end of nTMS), however, was rare (5%) and never remained for longer than 6 hr. No further side effects for example, seizures were observed for any of the modalities (nTMS, fMRI, DCS).

3.3 | Feasibility and robustness

3.3.1 | fMRI

The technical feasibility of fMRI was excellent. Except for one patient (tongue representation), all regions of interest could be identified in the entire group of patients.

NTMS: The feasibility of nTMS was 100% for the hand representation. Regarding the leg area, mapping could be performed at rest in 90% of the cases. In the remaining cases (10%), in which the RMT exceeded maximum stimulator output intensity, reasonable results could be achieved using pre-innervation (flexing toes). Face mapping was feasible at rest in 83% of the patients. Pre-innervation (pursing lips) was required in 13% of the patients. In one patient (3%), the exam was terminated due to transient pain, likely associated with direct stimulation of trigeminal nerve fibres in the stimulated area.

3.3.2 | DCS

Reliable and accurate DCS results could be obtained in $n = 25$ (69%) of the patients. The remaining 11/36 patients had to be excluded from further analysis of the DCS data due to different reasons: inaccurate neuronavigation ($n = 2$), small size of craniotomy and additional anatomical obstacles, for example, bridging veins impeding probe positioning over the respective cortical area ($n = 1$), no suitable MEP recordings due to motor threshold exceeding the maximum stimulation intensity or stimulation artefacts interfering with face muscle recordings ($n = 3$), technical problems during intraoperative data acquisition ($n = 5$), including data loss due to forced shutdown of the stimulator ($n = 2$).

Regarding somatotopic DCS mapping, reliable MEPs could be recorded from the hand representation in all cases when exposed by the craniotomy but was only possible in $N = 8/11$ (73%) patients with intended leg area mapping due to anatomical obstacles. Recording face muscle MEPs was challenging, mainly due to interference of the short-latency potentials with the stimulation artefact. In consequence, only $n = 13$ (65%) of the 20 intended face mappings could be included in the final analysis.

3.4 | Statistical congruency of functional maps

3.4.1 | Map centres

Comparison between fMRI and nTMS, relative to DCS: A three-factorial ANOVA with the factors MODALITY (two levels: ED [fMRI↔DCS], ED[TMS↔DCS]), CENTRE (two levels: hotspot, CoG) and SOMATOTOPY (three levels: hand, foot, tongue) on the respective EDs revealed a significant main effect of MODALITY ($F_{1,148} = 8.370$, $p < .01$) but no major effect of CENTRE or SOMATOTOPY. Interactions were not significant. Hence, ED(TMS↔DCS) were generally shorter than ED(fMRI↔DCS), thus suggesting a better agreement of the map centre detection with DCS for nTMS (mean ED = 11.4 ± 8.3 mm) as compared with fMRI (mean ED = 16.8 ± 7.0 mm; $p < .001$; Figure 2), irrespective of body part or centre estimation method. The additional analysis of the relative a.-p. location of fMRI versus DCS hotspots revealed a significantly more posterior location for the tongue area but not for the hand or foot hotspot or for any CoG. Likewise, there was no significant difference in the a.-p. location between DCS and TMS hotspots or CoGs (Table S3).

Congruency between fMRI and nTMS results: A two-factorial ANOVA with the factors CENTRE and SOMATOTOPY on ED [fMRI↔TMS] showed a significant main effect of the factor SOMATOTOPY ($F_{2,172} = 5.394$, $p = .005$) but no main effect or interaction regarding the factor CENTRE. The main effect of SOMATOTOPY was driven by significantly larger EDs for the tongue area as compared with both the hand and the foot representation (hand: 15.0 ± 8.4 mm; foot: 15.5 ± 9.0 mm; tongue: 20.1 ± 10.3 mm; $p \leq .01$). Of note, fMRI hotspots and CoGs were located significantly more posteriorly (along the y-axis) than the respective TMS hotspots/CoGs for the hand and the tongue area ($p \leq .05$, FDR-corrected). However, no significant difference was found for the foot area (Table S3).

3.5 | Map extents

Comparison between fMRI and nTMS, relative to DCS: A two-factorial ANOVA with the factors MODALITY (two levels: fMRI∩DCS, nTMS∩DCS) and SOMATOTOPY (three levels: hand, foot, tongue) was computed on the Dice coefficient as a measure of spatial congruency. This analysis revealed a significant main effect of both MODALITY ($F_{1,60} = 29.900$, $p < .001$) and SOMATOTOPY ($F_{2,60} = 3.178$, $p < .05$) but no interaction effect. Thus, spatial agreement with DCS was influenced by both the somatotopic region of interest and the non-invasive mapping method, driven by significantly higher Dice coefficients for nTMS compared with fMRI ($p < .001$).

The relative overlap volumes—normalised to the size of the DCS area – showed a better overlap for nTMS∩DCS as compared with fMRI∩DCS for all somatotopic maps (64 ± 38% vs. 37 ± 37%; $p < .01$) as well as regarding the hand area (60 ± 38% vs. 37 ± 39%; $p < .05$; FDR-corrected) and the foot region (57 ± 41% vs. 14 ± 14%; $p < .05$; FDR-corrected). In contrast, the difference in tongue area overlaps was not significant (73 ± 37% vs. 59 ± 39%; Figure 3a).

Accordingly, the detection rate of nTMS in terms of DCS-confirmed motor function was rather good, that is, the entire DCS map was completely included in the nTMS area in 52% (of functional regions) and showed at least partial overlap in 94% of the regions. In contrast, full inclusion of DCS data points in the fMRI area was only given for 18% of the areas whereas one third of DCS areas showed no overlap at all (Table 2). In comparison, the overall performance of

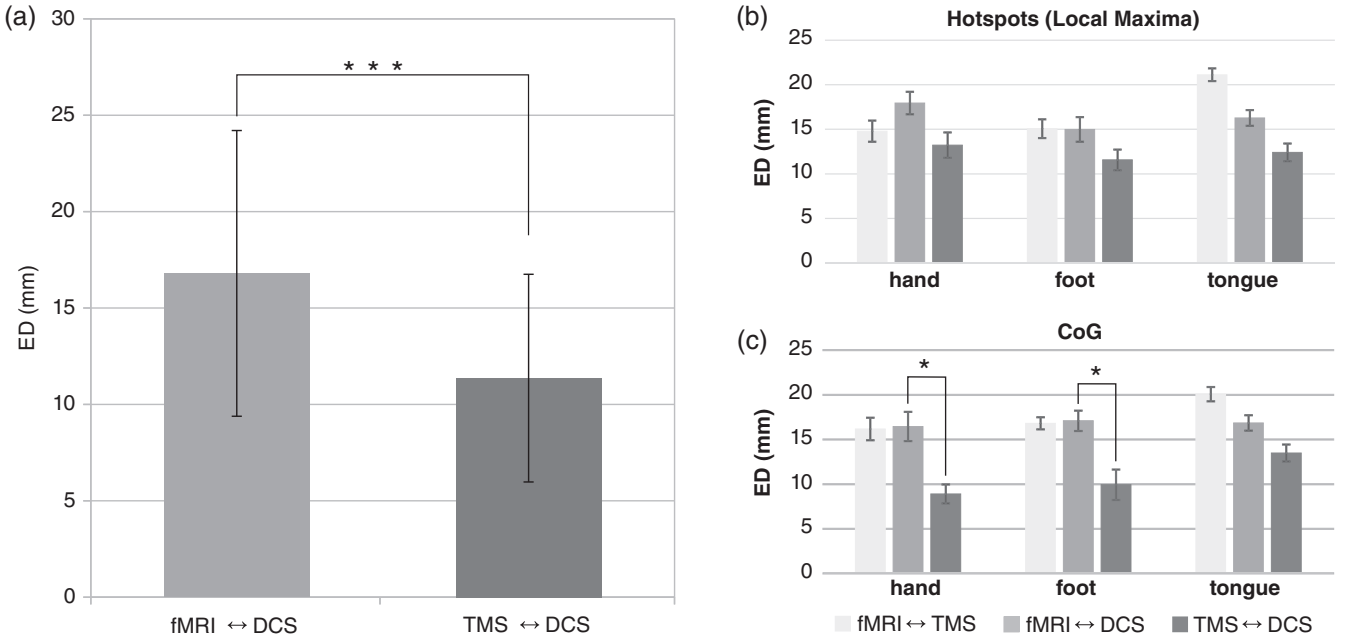

FIGURE 2 Distances between map centres. Euclidean distances (ED) between the respective pairs of 3D coordinates, representing (a) pooled data, (b) hotspots/local activation maxima and (c) CoG. Pairs of modalities are colour-encoded: ED between fMRI and nTMS (light grey), between fMRI and DCS (grey) as well as between nTMS and DCS (dark grey). In A, statistically significant differences between ED according to post hoc tests are indicated by asterisks (*p < .05; ***p < .001). Error bars represent *SEM*

nTMS to detect the functional DCS area was better than for fMRI (p < .01; Table 3).

Congruency between fMRI and nTMS results: The mean overlap between the surface-projected fMRI and nTMS maps was 23 ± 21%. One-factorial ANOVA revealed no significant effect of the factor SOMATOTOPY (Figure 3b).

4 | DISCUSSION

Intraoperative mapping and monitoring is still the gold standard for neurosurgery in motor-eloquent brain regions. However, additional non-invasive function localization can help to overcome the procedural limitations of DCS. We found better mapping results for nTMS compared with fMRI for both map centres and map extents, as expressed by ED and relative overlap volumes, in a comparatively large consecutive cohort of patients (see Table 4 for comparison).

4.1 | Clinical outcome and relevance of perioperative mapping

The increasing use of non-invasive mapping techniques for preoperative diagnostics has been accompanied by a change in the tumour resection strategy towards a more quality-of-life-oriented, function-preserving surgical approach over the last decades. As compared with historical cohorts from the 1980s to early 2000s with rates of surgery-related deterioration of motor function in the range of 60% (transient; 26–38% permanent) (Magill, Han, Li, & Berger, 2018; Raffa et al., 2018), resection of motor-eloquent brain tumours has become safer since more effort has been made to assess the functional limits of MC areas for surgery using non-invasive methods: with 35% transient and 5% permanent surgery-related motor deficits, the outcome results of the glioma patients in our cohort agree relatively well with the recent literature reporting new postoperative motor deficits in the range of 23–29% (transient) versus 8–22% (permanent) after nTMS- and DCS-guided resection of motor-eloquent gliomas (Hendrix et al., 2016; Rosenstock et al., 2017; Sollmann et al., 2018). However, the relatively high percentage of transient motor deficits in our cohort might be a consequence of considering (even mild) isolated face muscle impairments as surgery-related motor deficit (n = 4, that is, 20% of all patients). As opposed to motor deficits of the limbs, central facial palsy usually recovers comparatively well due to good neuroplastic capabilities, linked to the far more considerable bilateral supply via uncrossed corticobulbar projections (Duffau, Capelle, Denvil, & Van Effenterre, 2003; Neuloh & Clusmann, 2011; Pilurzi et al., 2013). Since the type of tumour entity, particularly gliomas versus non-glial tumours, probably has a relevant influence on the functional outcome (Hendrix et al., 2016; Sollmann et al., 2018), we did not pool outcome data from different histological cohorts.

Apart from improved preservation of motor function, it has been hypothesised that the extent of resection might be higher in cohorts with additional preoperative nTMS motor mapping compared with intraoperative DCS alone (e.g., Krieg et al., 2014). In the present study population, a GTR of 55% could be achieved for patients with gliomas (°II–°IV) which is in line with previous publications on both

nTMS-guided (Rosenstock et al., 2017) and solely DCS-guided (Magill et al., 2018) glioma surgery which found GTR rates of approximately 50%. Again, comparison of the mixed group resection outcome (i.e., 59% GTR in our cohort) with previous studies reporting GTR rates from 52 to 78% (Krieg et al., 2014; Raffa et al., 2018) is difficult due to the heterogeneity of histological entities, influencing the surgical strategy.

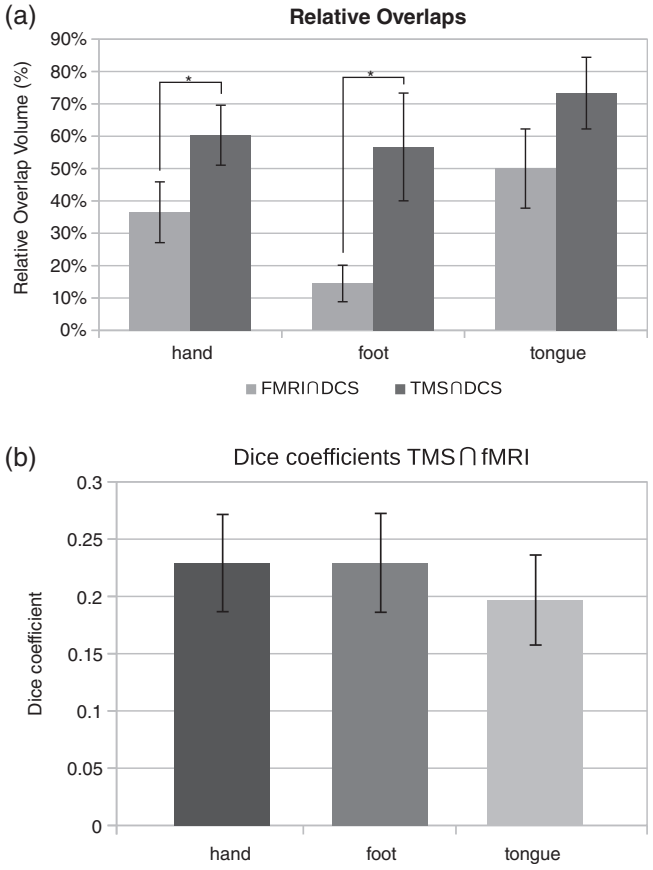

FIGURE 3 Congruency of map extents. (a) Relative overlaps (normalised to the respective DCS area) between functional areas, assessed by different modalities. Modality pairs are colour-encoded (light grey: fMRI∩DCS/DCS, dark grey: nTMS∩DCS/DCS). (b) Dice coefficients of fMRI∩TMS. For both (a) and (b), statistically significant differences are indicated by asterisks (*p < .05, FDR-corrected). Error bars represent *SEM*

4.2 | Accuracy of non-invasive motor function methods

4.2.1 | Map centres

We observed a better accuracy of nTMS versus fMRI for map centres, going along with a generally more posterior location of fMRI map centres in comparison to nTMS. The relatively posterior location of the fMRI map centres agrees with previous publications for example, by Diekhoff et al. (2011) and could be at least partly explained by the not fully evitable somatosensory coactivation inherent to active motor tasks (Blatow et al., 2011). In line with our findings regarding the direct comparison of fMRI and nTMS map centre locations with DCS, better agreement of the nTMS hotspots with DCS has been reported previously. Overall, the results of our study on the hotspots of nTMS↔DCS (hand: 13.23 ± 9.37, foot: 11.57 ± 7.77) and fMRI↔DCS (hand: 17.95 ± 10.57, foot: 14.99 ± 7.19) were comparable with the findings of other groups. For the hand area, nTMS↔DCS distances were reported to range between 9.5 and 14.4 mm, whereas distances for fMRI↔DCS centres were between 11.6 and 18.2 mm (Forster et al., 2011; Mangraviti et al., 2013). The shortest distances between nTMS↔DCS results were reported by Krieg et al. (2012) who found ED of 4.4 ± 4 mm between the margins of the functional areas in a two-dimensional analysis on axial screenshots. For the foot area, ED from 7.8 to 11.0 mm were reported for nTMS↔DCS hotspots and from 10.9 to 12.00 mm for fMRI↔DCS (Forster et al., 2011, Mangraviti et al., 2013). Direct comparison, however, is difficult, for example, due to different centre estimation methods (Table 4). In this study, ED between nTMS/fMRI and DCS tongue map centres were in a similar range compared with the other somatotopies.

4.3 | Map extents

On average, the agreement of nTMS areas with DCS was better in comparison to fMRI, as expressed by higher relative overlap volumes. This finding was confirmed for the somatotopic representations of the hand and the foot as well as, overall, by the semiquantitative analysis, revealing a higher percentage of complete detection of DCS-positive stimulation sites using nTMS rather than fMRI. Here, the relatively poor agreement of fMRI clusters with DCS data compared with nTMS is likely related to changes in neurovascular coupling in the vicinity of

TABLE 2 Semiquantitative coverage of DCS areas by non-invasive functional localizer results

DCS area included		fMRI				nTMS			
		Hand	Foot	Tongue	All	Hand	Foot	Tongue	All
Complete	*n* (percentage)	2 (13%)	0 (0%)	4 (36%)	6 (18%)	8 (50%)	3 (50%)	6 (55%)	17 (52%)
Partial	*n* (percentage)	9 (56%)	2 (33%)	5 (45%)	16 (48%)	6 (38%)	3 (50%)	5 (45%)	14 (42%)
Not at all	*n* (percentage)	5 (31%)	4 (67%)	2 (18%)	11 (33%)	2 (13%)	0 (0%)	0 (0%)	2 (6%)

Note: Counts and percent of total are given for fMRI and nTMS, grouped by body parts and overall (columns). Detection rate regarding the DCS area extents was classified in complete (100%), partial and no coverage (rows).

TABLE 3 Contingency table showing count data distribution of nTMS versus fMRI agreement with DCS map extents

Inclusion of DCS area		nTMS			
		None	Partial	Complete	Any
fMRI	None	1	4	6	*11*
	Partial	1	9	6	*16*
	Complete	0	1	5	*6*
	Any	*2*	*14*	*17*	*33*

Note: Overall, nTMS showed higher detection potential compared with fMRI (McNemar Chi-squared test; $p < .001$).

cerebral mass lesions and oedema (e.g., Hoefnagels et al., 2014; Lu, Ahn, Johnson, & Cha, 2003). Similar effects were found using fMRI as an origin localizer technique in DTI-based tractography on the tumour hemisphere (Weiß Lucas et al., 2017). Moreover, the rather deeply located functional foot representation along the median longitudinal fissure (Catani, 2017) challenges surface projection algorithms, possibly reducing the agreement of fMRI with DCS for this somatotopic region. In addition, the similarity of the nTMS action mechanism to DCS, that is, exciting both neurons and superficial white matter fibres, could qualify the method as a better estimate of the gold standard results, as compared with fMRI which makes use of a vascular signal. To the best of our knowledge, Opitz et al. (2014) provide the only previous data comparing functional area extents assessed by nTMS versus DCS, reporting a relative overlap of up to 80% for the hand representation. However, comparability is clearly confounded by several major differences in methodology; for example, DCS was applied only over the precentral gyrus (stimulation sites spaced by ~5 mm) and nTMS mappings were restricted to 5 mm-spaced grid points centred around the hotspot. In contrast, we mapped the entire, accessible extent of the functional region. Moreover, the results reported by Opitz and colleagues were based on computational modelling of the electric field, using different models (spherical vs realistic) and threshold levels for nTMS, whereas our intention was to test the accuracy of nTMS versus fMRI under standard post-processing conditions. Of note, both model and threshold had a strong influence on the results of Opitz and colleagues, with overlaps in the range of 0–45% (spherical model) versus 0–80% (realistic model), increasing with maximum electric field strength.

4.4 | Agreement between nTMS and fMRI map centres

In our patient cohort, the distances between nTMS↔fMRI hotspots of the hand area (14.8 ± 8.3 mm) were comparable to the results from healthy subjects (13.5 ± 2.0 mm) based on the same paradigms (Weiss et al., 2013). However, the higher variance of distances in this study might reflect the increased methodological challenge of non-invasive mapping in tumour patients, for example, due to the limitation of fMRI signal detection in the neighbourhood of cerebral mass lesions discussed above or the effect of antiepileptic drugs. In the light of previous studies, the EDs found for the different body part representations were in the medium range, reaching from 6.3 to 24.3 mm (Forster et al., 2011; Krieg et al., 2012; Mangraviti et al., 2013; Picht et al., 2011).

Here, we also found a significant influence of the somatotopy of interest on the ED between fMRI↔TMS ($p < .01$). Highest ED were observed for the tongue area (20.1 ± 10.3 mm; $p \leq .01$). The comparatively high distances might be partly due to the relatively large cortical area occupied by the tongue representation, which often includes more than one local activation maximum. Moreover, as compared with other body parts, tongue movement is more prone to head movement artefacts in fMRI.

4.5 | Limitations

Although this study represents, to the best of our knowledge, the largest series comparing nTMS motor cortex mappings to DCS, the number of comparisons of fMRI versus nTMS to DCS was limited by the extent of the craniotomy, hence, the intraoperatively exposed functional area and procedural challenges. This affected particularly the foot representation where the anatomical access to the cortex near the midline allowed the acquisition of a comprehensive DCS map in only six patients. Since we found a significant influence of the area of interest on the Dice coefficients, the problem of a relatively low number per somatotopic area affected the overlap analysis. However, post hoc effect size and power calculation revealed an acceptable power for all areas, despite the comparatively low sample size. Accordingly, we found a statistical power of at least 0.7 for all areas (hand: 0.997; foot: 0.866; tongue: 0.668; two-sided) due to the high effect sizes in the overlap analysis (hand: d = 1.265; foot: d = 1.578; tongue: d = 0.800).

The generally more posterior location of the fMRI hotspots/CoGs relative to the TMS hotpots/CoGs (but in most of the cases not relative to DCS) might have been influenced by smoothing including an isotropic Gaussian kernel. This approach was chosen to allow for optimal comparability of our results with daily practice, especially regarding clinical diagnostics (see e.g., Rosazza et al., 2014) but might have been at the cost of a certain loss of information regarding the spatial extent and the shape of the activation area. Using alternative preprocessing procedure such as surface based analysis (Anticevic et al., 2008; Jo et al., 2007), structure adaptive smoothing (Tabelow, Polzehl, Voss, & Spokoiny, 2006) or a spatially adaptive conditionally autoregressive modelling (Liu, Berrocal, Bartsch, & Johnson, 2016) might have led to a better agreement of both fMRI and nTMS map centres also in the y-axis.

Due to the methodological differences between nTMS, fMRI and DCS, comparability of map extents and centres had to be optimised post hoc: functional sites identified by each modality were projected onto the same brain level, that is, the cortical surface where DCS naturally occurs. Of note, DCS data had to be projected back onto the original cortical surface in case of brain shift or swelling. Although we consider this approach (using an observer-independent Matlab script

TABLE 4 Current evidence regarding the accuracy of non-invasive mapping including nTMS for brain tumour patients

Author, year	n of subjects with DCS data (overall)	Histology	Non-invasive modalities			Somatotopic regions compared with DCS			Congruency measures			
									Euclidean distances (ED) in mm			
			nTMS	fMRI	MEG	Hand/arm	Foot/leg	Face/tongue	Hotspot (3D)	CoG (3D)	Others (2D)	Overlap relative to DCS
Picht et al., 2011	17(20)	Mixed	x			x	x		APB 7.8 ± 1.2; TA 7.1 ± 0.9 (SEM)			
Forster et al., 2011	9(10)[a]	Mixed	x	x		x	x		nTMS: APB 14.4 ± 8.7; ExtDigg 12.1 ± 3.6; TA 11.0 ± 5.6			
Krieg et al., 2012	14(26)	Mixed	x	x		x	x				nTMS[b]: 4.4 ± 4.3; fMRI: Not reported	
Tarapore et al., 2012	5(24)	Glioma	x		x	x			nTMS APB/ADM: 2.1 ± 0.3; MEG: 12.1 ± 8.2 (*SEM*)			
Paiva et al., 2012	6(6)	Glioma	x			x					"Hand"[c]:4.16 ± 1.02	
Mangraviti et al., 2013	7(8)	Mixed	x	x		x	x		nTMS: APB 9.5 ± 5.2; FCR 7.9 ± 4.2; TA 7.8 ± 3.7 (CI)	fMRI[d]: APB 11.6 ± 4.0; FCR: 14.0 ± 6.4; TA 12.0 ± 9.9 (CI)		
Opitz, Zafar, Bockermann, Rohde, & Paulus, 2014	6(6)	Mixed	x	x		x				FDI[e]: 9.4 ± 1.5 (*SEM*)		80%[e]
Seynaeve et al., 2019	6/12(12)[f]	Mixed	x			x	x			APB/TA: 11 ± 1.5[e]		
THIS STUDY	25(36)	Mixed	x	x		x	x	x	nTMS APB/TA/tongue: 12.6 ± 8.6; fMRI: 16.8 ± 9.7 ($p < .05$)	nTMS APB/TA/tongue: 10.5 ± 8.3; fMRI: 16.7 ± 9.6 ($p < .001$)		nTMS APB/TA/tongue: 64 ± 38%; fMRI: 37 ± 37% ($p < .01$)

Note: [a]One subject included twice in the study due to repeated surgery, thus 10(11) mapping comparisons.
[b]Distances between margins of functional areas measured in 2D (axial screen shots), all muscles/regions pooled: APB/ADM/biceps/TA/gastrocnemius.
[c]Referred to as "geometric centres."
[d]Referred to as "centre of fMRI activation area."
[e]For best fitting (realistic) computational E-field model.
[f]Six DCS mappings with more than one data point.
Abbreviations: ADM, abductor digiti minimi muscle; APB, abductor pollicis brevis muscle; ExtDigg, extensor digitorum muscle; FCR, flexor carpi radialis muscle; FDI, first dorsal interosseous muscle; TA, anterior tibial muscle.

for surface projection) as most reliable, a certain confound is inevitably introduced by applying post-processing to the coordinates. Intraoperative MRI would allow for more accurate detection of the DCS sites after dural opening. However, considering the risk–benefit ratio of the study, adding 1 hr (Senft et al., 2011) for unplanned, not clinically indicated scans (before starting tumour resection) plus an increased risk of general complications due to prolonged anaesthesia and a variety of management concerns (see Berkow, 2016 for review), did not justify the minor improvement in data quality.

Finally, comparability of the three mapping methods—nTMS, fMRI and DCS—remains limited by their different methodologies which make none of the methods perfectly suited to specifically map the primary motor cortex proper. Whereas fMRI activation is influenced i.a. by the local cerebral blood flow alterations and the distinct sensorimotor and secondary-motor components of the task, nTMS acts primarily on white matter projections especially in regions of fibre bending instead of activating the pyramidal cell bodies in layer Vb. Here, identification of unspecific activations (fMRI)/MEPs (nTMS, DCS) by sole addition of morpho-anatomical information, that is, considering the traditional boundaries of Brodmann area 4, does not seem appropriate since even in healthy subjects the functional motor representation and its micromorphological correlates underlie a significant intra- and interindividual variability, often even exceeding the precentral gyrus (Kumar et al., 2009; Rademacher et al., 2001; Rivara, Sherwood, Bouras, & Hof, 2003; Toyoshima & Sakai, 1982). This uncertainty regarding the estimated representation of the primary motor cortex proper is further enhanced in the presence of brain lesions like oedema or tumours which drive functional plasticity, especially on cortex level (see also Duffau, 2014 for review).

5 | CONCLUSIONS

Precise non-invasive motor mapping techniques are of great importance to ensure conscious decision-making and can help to achieve safe but maximal tumour removal. Beyond supporting the previous evidence that nTMS-determined centre coordinates of motor areas in the neighbourhood of brain tumours agree better with the intraoperative DCS as compared with fMRI, our results add the important finding that the spatial extent of the functional map is also delineated more accurately by nTMS, irrespective of the addressed somatotopic region, even considering the technically more challenging face/tongue mappings. The clinical outcome in this high-risk cohort of patients with tumours near the central region demonstrate a good overall trade-off between surgical outcome (with significant impact on survival) and postoperative motor functions. Interestingly, an additional exploratory analysis revealed very similar rates of surgery-related motor deficits comparing the groups of patients with difficult or incomplete intraoperative DCS (due to procedural complications) to patients with comprehensive DCS mappings. Although the study was not sufficiently powered to analyse factors on rare events such as permanent deficits, this finding could be interpreted as an indication of at least partial compensation for limited DCS feasibility by the generally more robust non-invasive mapping. However, not only due to the cumulative imprecision inherent in computational models and co-registration systems but also by the increased brain shift associated with dural opening and tumour/tissue removal, non-invasive techniques should be regarded as a valuable addition to intraoperative DCS—although based on the presented evidence a substitution of intraoperative mapping and monitoring is not indicated.

ACKNOWLEDGEMENTS

We thank the MR staff of Forschungszentrum Jülich for their support. CWL and RG received funding from the German Research Foundation (DFG) (INST 1856/50-1). CWL received additional funding from the Faculty of Medicine of the University of Cologne (Koeln Fortune/Gerok 8/2016).

CONFLICT OF INTERESTS

The authors have no conflicts of interest to disclose.

DATA AVAILABILITY STATEMENT

The data that support the findings of this study are available on reasonable request from the corresponding author, C. W. L.

ORCID

Carolin Weiss Lucas https://orcid.org/0000-0001-6463-0034
Volker Neuschmelting https://orcid.org/0000-0001-7527-6990
Gabriele Stoffels https://orcid.org/0000-0001-7114-1941
Shivakumar Viswanathan https://orcid.org/0000-0002-7513-3778
N. Jon Shah https://orcid.org/0000-0002-8151-6169
Karl Josef Langen https://orcid.org/0000-0003-1101-5075
Christian Grefkes https://orcid.org/0000-0002-1656-720X

REFERENCES

Anticevic, A., Dierker, D. L., Gillespie, S. K., Repovs, G., Csernansky, J. G., Van Essen, D. C., & Barch, D. M. (2008). Comparing surface-based and volume-based analyses of functional neuroimaging data in patients with schizophrenia. *NeuroImage*, *41*(3), 835–848.

Benjamini, Y., & Hochberg, Y. (1995). Controlling the false discovery rate: A practical and powerful approach to multiple testing. *Journal of the Royal Statistical Society: Series B*, *57*, 289–300.

Berkow, L. C. (2016). Anesthetic management and human factors in the intraoperative MRI environment. *Current Opinion in Anaesthesiology*, *29*(5), 563–567.

Blatow, M., Reinhardt, J., Riffel, K., Nennig, E., Wengenroth, M., & Stippich, C. (2011). Clinical functional MRI of sensorimotor CortexUsing passive motor and sensory stimulation at 3 tesla. *Journal of Magnetic Resonance Imaging*, *34*, 429–437.

Bonhomme, V., Franssen, C., & Hans, P. (2009). Awake craniotomy. *European Journal of Anaesthesiology*, *26*(11), 906–912.

Catani, M. (2017). A little man of some importance. *Brain*, *140*(11), 3055–3061.

Deiber, M. P., Passingham, R. E., Colebatch, J. G., Friston, K. J., Nixon, P. D., & Frackowiak, R. S. (1991). Cortical areas and the selection of movement: A study with positron emission tomography. *Experimental Brain Research*, *84*(2), 393–402.

Desmurget, M., & Sirigu, A. (2015). Revealing humans' sensorimotor functions with electrical cortical stimulation. *Philosophical Transactions of the Royal Society, B: Biological Sciences*, *370*(1677), 20140207.

Dice, Lee R. (1945). Measures of the Amount of Ecologic Association Between Species. *Ecology*, *26*(3), 197–302.

Diekhoff, S., Uludağ, K., Sparing, R., Tittgemeyer, M., Cavuşoğlu, M., von Cramon, D. Y., & Grefkes, C. (2011). Functional localization in the human brain: Gradient-Echo, spin-Echo, and arterial spin-labeling fMRI compared with neuronavigated TMS. *Human Brain Mapping*, *32*(3), 341–357.

Duffau, H. (2014). The huge plastic potential of adult brain and the role of connectomics: New insights provided by serial mappings in glioma surgery. *Cortex*, *58*, 325–337.

Duffau, H., Capelle, L., Denvil, D., & Van Effenterre, R. (2003). Functional recovery after surgical resection of low grade gliomas in eloquent brain: Hypothesis of brain compensation. *JNNP Journal of Neurology Neurosurgery & Psychiatry*, *74*(7), 901–907.

Forster, M. T., Hattingen, E., Senft, C., Gasser, T., Seifert, V., & Szelényi, A. (2011). Navigated transcranial magnetic stimulation and functional magnetic resonance imaging: Advanced adjuncts in preoperative planning for central region Tumours. *Neurosurgery*, *68*(5), 1317–1324.

Gallen, C. C., Schwartz, B. J., Buchholz, R. D., Malik, G., Garkley, G. L., Smith, J., … Bloom, F. (1995). Presurgical localization of functional cortex using magnetic source imaging. *Journal of Neurosurgery*, *82*(6), 988–994.

Gil-Robles, S., & Duffau, H. (2010). Surgical management of World Health Organization grade II gliomas in eloquent areas: The necessity of preserving a margin around functional structures. *Neurosurgical Focus*, *28* (2), E8.

Hemmerling, T. M., & Le, N. (2007). Neuromuscular monitoring: An update for the clinician. *Canadian Journal of Anaesthesiology*, *54*(1), 58–72.

Hendrix, P., Senger, S., Griessenauer, C. J., Simgen, A., Schwerdtfeger, K., & Oertl, J. (2016). Preoperative navigated transcranial magnetic stimulation in patients with motor eloquent lesions with emphasis on metastasis. *Clinical Anatomy*, *29*(7), 925–931.

Hoefnagels, F. W. A., De Witt Hamer, P., Sanz-Arigita, E., Idema, S., Kuijer, J. P., Pouwels, P. J., … Vandertop, W. P. (2014). Differentiation of edema and glioma infiltration: Proposal of a DTI-based probability map. *Journal of Neurooncology*, *120*(1), 187–198.

House, J. W., & Brackmann, D. E. (1985). Facial nerve grading system. *Otolaryngology–Head and Neck Surgery*, *93*(2), 146–147.

Jo, H. J., Lee, J. M., Kim, J. H., Shin, Y. W., Kim, I. Y., Kwon, J. S., & Kim, S. I. (2007). Spatial accuracy of fMRI activation influenced by volume- and surface-based spatial smoothing techniques. *NeuroImage*, *34*(2), 550–564.

Karnofsky, D. A., & Burchenal, J. H. (1949). The clinical evaluation of chemotherapeutic agents in cancer. In C. M. MacLeod (Ed.), *Evaluation of chemotherapeutic agents*. New York: Columbia Univ Press.

Kober, H., Nimsky, C., Möller, M., Hastreiter, P., Fahlbusch, R., & Ganslandt, O. (2001). Correlation of sensorimotor activation with functional magnetic resonance imaging and magnetoencephalography in presurgical functional imaging: A spatial analysis. *NeuroImage*, *14*(5), 1214–1228.

Korvenoja, A., Kirveskari, E., Aronen, H. J., Avikainen, S., Brander, A., Huttunen, J., … Seppä, M. (2006). Sensorimotor cortex localization: Comparison of magnetoencephalography, functional MR imaging, and intraoperative cortical mapping. *Radiology*, *241*(1), 213–222.

Krieg, S. M., Sabih, J., Bulubasova, L., Obermueller, T., Negwer, C., Janssen, I., … Ringel, F. (2014). Preoperative motor mapping by navigated transcranial magnetic brain stimulation improves outcome for motor eloquent lesions. *Neuro-Oncology*, *16*(9), 1274–1282.

Krieg, S. M., Shiban, E., Buchmann, N., Gempt, J., Foerschler, A., Meyer, B., & Ringel, F. (2012). Utility of presurgical navigated transcranial magnetic brain stimulation for the resection of tumors in eloquent motor areas. *Journal of Neurosurgery*, *116*(5), 994–1001.

Kumar, A., Juhasz, C., Asano, E., Sundaram, S. K., Makki, M. I., Chugani, D. C., & Chugani, H. T. (2009). Diffusion tensor imaging study of the cortical origin and course of the corticospinal tract in healthy children. *AJNR. American Journal of Neuroradiology*, *30*(10), 1963–1970.

Lefaucheur, J. P., & Picht, T. (2016). The value of preoperative functional cortical mapping using navigated TMS. *Clinical Neurophysiology*, *46*(2), 125–133.

Liu, Z., Berrocal, V. J., Bartsch, A. J., & Johnson, T. D. (2016). Pre-surgical fMRI data analysis using a spatially adaptive conditionally autoregressive model. *Bayesian Analysis*, *11*(2), 599–625.

Lu, S., Ahn, D., Johnson, G., & Cha, S. (2003). Peritumoral diffusion tensor imaging of high-grade gliomas and metastatic brain tumors. *AJNR. American Journal of Neuroradiology*, *24*, 937–941.

Magill, S. T., Han, S. J., Li, J., & Berger, M. S. (2018). Resection of primary motor cortex tumors: Feasibility and surgical outcomes. *Journal of Neurosurgery*, *129*(4), 961–972.

Mangraviti, A., Casali, C., Cordella, R., Legnani, F. G., Mattei, L., Prada, F., … DiMeco, F. (2013). Practical assessment of preoperative functional mapping techniques: Navigated transcranial magnetic stimulation and functional magnetic resonance imaging. *Neurological Sciences*, *34*(9), 1551–1557.

McNemar, Q. (1947). Note on the sampling error of the difference between correlated proportions or percentages. *Psychometrika*, *12*(2), 153–157.

Medical Research Council. (1976). *Aids to examination of the peripheral nervous system. Memorandum no. 45*. London: Her Majesty's Stationary Office.

Neuloh, G., Clusmann, H. (2011). Resection of the primary face motor area in brain tumors. Paper presented as Meeting Abstract at the Annual Meeting of the German Society of Neurosurgery (DGNC), Hamburg. https://doi.org/10.3205/11dgnc290

Opitz, A., Zafar, N., Bockermann, V., Rohde, V., & Paulus, W. (2014). Validating computationally predicted TMS stimulation areas using direct electrical stimulation in patients with brain tumors near precentral regions. *Neuroimage:Clinical*, *18*(4), 500–507.

Paiva, Wellington S., Fonoff, Erich T., Marcolin, Marco A., Cabrera, Hector N., & Teixeira, Manoel J. (2012). Cortical Mapping With Navigated Transcranial Magnetic Stimulation in Low-Grade Glioma Surgery. *Neuropsychiatr Dis Treat*, *8*, 197–201.

Picht, T., Schmidt, S., Brandt, S., Frey, D., Hannula, H., Neuvonen, T., … Suess, O. (2011). Preoperative functional mapping for rolandic brain tumor surgery: Comparison of navigated transcranial magnetic stimulation to direct cortical stimulation. *Neurosurgery*, *69*(3), 581–588.

Pilurzi, G., Hasan, A., Saifee, T. A., Tolu, E., Rothwell, J. C., & Deriu, F. (2013). Intracortical circuits, sensorimotor integration and plasticity in human motor cortical projections to muscles of the lower face. *The Journal of Physiology*, *591*(7), 1889–1906.

Preparata, F. P., & Shamos, M. I. (1985). *Computational geometry: An introduction*. New York: Springer.

Rademacher, J., Bürgel, U., Geyer, S., Schormann, T., Schleicher, A., Freund, H. J., & Zilles, K. (2001). Variability and asymmetry in the human precentral motor system. A cytoarchitectonic and myeloarchitectonic brain mapping study. *Brain*, *124*(11), 2232–2258.

Raffa, G., Conti, A., Scibilia, A., Cardali, S. M., Esposito, F., Angileri, F. F., … Tomasello, F. (2018). The impact of diffusion tensor imaging fiber tracking of the corticospinal tract based on navigated transcranial magnetic stimulation on surgery of motor-eloquent brain lesions. *Neurosurgery*, *83*(4), 768–782.

Reinges, M. H., Krings, T., Meyer, P. T., Schreckenberger, M., Rohde, V., Weidemann, J., … Gilsbach, J. M. (2004). Preoperative mapping of cortical motor function: Prospective comparison of functional magnetic resonance imaging and [15O]-H2O-positron emission tomography in the same co-ordinate system. *Nuclear Medicine Communications*, *25* (10), 987–997.

Rivara, C.-B., Sherwood, C. C., Bouras, C., & Hof, P. R. (2003). Stereologic characterization and spatial distribution patterns of Betz cells in the human primary motor cortex. *The Anatomical Record Part A*, *270A*, 137–151.

Rosazza, C., Aquino, D., D'Incerti, L., Cordella, R., Andronache, A., Zacà, D., … Minati, L. (2014). Preoperative mapping of the sensorimotor cortex: Comparative assessment of task-based and resting-state fMRI. *PLoS ONE*, *9*(6), e98860. https://doi.org/10.1371/journal.pone.0098860

Rosenstock, T., Grittner, U., Acker, G., Schwarzer, V., Kulchytska, N., Vajkoczy, P., & Picht, T. (2017). Risk stratification in motor area-related glioma surgery based on navigated transcranial magnetic stimulation data. *Journal of Neurosurgery*, *126*(4), 1227–1237.

Scheufler, K. M., & Zentner, J. (2002). Total intravenous anesthesia for intraoperative monitoring of the motor pathways: An integrated view combining clinical and experimental data. *Journal of Neurosurgery*, *96*, 571–579.

Senft, C., Bink, A., Franz, K., Vatter, H., Gasser, T., & Seifert, V. (2011). Intraoperative MRI guidance and extent of resection in glioma surgery: A randomised, controlled trial. *Lancet Oncology*, *12*(11), 997–1003.

Seynaeve, L., Haeck, T., Gramer, M., Maes, F., De Vleeschouwer, S., & Van Paesschen, W. (2019). Optimized preoperative motor cortex mapping in brain tumors using advanced processing of transcranial magnetic stimulation data. *Neuroimage:Clinical*, *21*, 101657.

Shen, J. (2014). Tools for NifTI and ANALYZE image [MATLAB Central File Exchange]. Retrieved from https://www.mathworks.com/matlabcentral/fileexchange/8797-tools-for-nifti-and-analyze-image

Sloan, T. B. (1998). Anesthetic effects on Electrophysiologic recordings. *Journal of Clinical Neurophysiology*, *15*(3), 217–226.

Sollmann, N., Wildschuetz, N., Kelm, A., Conway, N., Moser, T., Bulubas, L., … Krieg, S. M. (2018). Associations between clinical outcome and navigated transcranial magnetic stimulation characteristics in patients with motor-eloquent brain lesions: A combined navigated transcranial magnetic stimulation–diffusion tensor imaging fiber tracking approach. *Journal of Neurosurgery*, *128*(3), 800–810.

Suess, O., Suess, S., Brock, M., & Kombos, T. (2006). Intraoperative electrocortical stimulation of Brodman area 4: A 10-year analysis of 255 cases. *Head & Face Medicine*, *2*, 20.

Szelényi, A., Bello, L., Duffau, H., Fava, E., Feigl, G. C., Galanda, M., … Sala, F. (2010). Intraoperative electrical stimulation in awake craniotomy: methodological aspects of current practice). Workgroup for intraoperative Management in low-Grade Glioma Surgery within the European low-grade glioma network. *Neurosurgical Focus*, *28*(2), E7.

Tabelow, K., Polzehl, J., Voss, H. U., & Spokoiny, V. (2006). Analyzing fMRI experiments with structural adaptive smoothing procedures. *NeuroImage*, *33*(1), 55–62.

Takahashi, S., Vajkoczy, P., & Picht, T. (2013). Navigated transcranial magnetic stimulation for mapping the motor cortex in patients with rolandic brain tumors. *Neurosurgical Focus*, *34*(4), E3.

Tarapore, P. E., Picht, T., Bulubas, L., Shin, Y., Kulchytska, N., Meyer, B., … Krieg, S. M. (2016). Safety and tolerability of navigated TMS for preoperative mapping in neurosurgical patients. *Clinical Neurophysiology*, *127*(3), 1895–1900.

Tarapore, P. E., Tate, M. C., Findlay, A. M., Honma, S. M., Mizuiri, D., Berger, M. S., & Nagarjan, S. S. (2012). Preoperative multimodal motor mapping: A comparison of magnetoencephalography imaging, navigated transcranial magnetic stimulation, and direct cortical stimulation. *Journal of Neurosurgery*, *117*(2), 354–362.

Toyoshima, K., & Sakai, H. (1982). Exact cortical extent of the origin of the corticospinal tract (CST) and the quantitative contribution to the CST in different cytoarchitectonic areas. A study with horseradish peroxidase in the monkey. *Journal für Hirnforschung*, *23*(3), 257–269.

Vidyasagar, R., & Parkes, L. M. (2011). Reproducibility of functional MRI localization within the human somatosensory cortex. *Journal of Magnetic Resonance Imaging*, *34*, 1439–1444.

Weiss, C., Nettekoven, C., Rehme, A. K., Neuschmelting, V., Eisenbeis, A., Goldbrunner, R., & Grefkes, C. (2013). Mapping the hand, foot and face representations in the primary motor cortex – Retest reliability of neuronavigated TMS versus functional MRI. *NeuroImage*, *66*, 531–542.

Weiss Lucas, C., Tursunova, I., Neuschmelting, V., Lockau, H., Nettekoven, C., Oros-Peusquens, A. M., … Grefkes, C. (2017). Functional MRI vs. navigated TMS to optimize M1 seed volume delineation for DTI tractography. A prospective study in patients with brain tumours adjacent to the corticospinal tract. *Neuroimage:Clinical*, *13*, 297–309.

SUPPORTING INFORMATION

Additional supporting information may be found online in the Supporting Information section at the end of this article.

How to cite this article: Weiss Lucas C, Nettekoven C, Neuschmelting V, et al. Invasive versus non-invasive mapping of the motor cortex. *Hum Brain Mapp*. 2020;1–14. https://doi.org/10.1002/hbm.25101